Molecular Phylogenetics and Evolution 127 (2018) 988–999

Contents lists available at ScienceDirect

Molecular Phylogenetics and Evolution

journal homepage: www.elsevier.com/locate/ympev

Species delimitation and mitogenome phylogenetics in the subterranean genus *Pseudoniphargus* (Crustacea: Amphipoda)

Morten Stokkan[a], José A. Jurado-Rivera[b], Pedro Oromí[c], Carlos Juan[a,b], Damià Jaume[a], Joan Pons[a,*]

[a] IMEDEA (CSIC-UIB), Mediterranean Institute for Advanced Studies, C/ Miquel Marquès 21, Esporles, 07190 Balearic Islands, Spain
[b] Dept. of Biology, Universitat de les Illes Balears, Ctra. Valldemossa km 7'5, Palma 07122, Balearic Islands, Spain
[c] Dept. of Animal Biology, Edaphology and Geology, Universidad de La Laguna, Avda. Astrofísico Francisco Sánchez, s/n. Campus de Anchieta, Ap. correos 456, La Laguna 38200, Tenerife, Spain

A B S T R A C T

The amphi-Atlantic distributions exhibited by many thalassoid stygobiont (obligate subterranean) crustaceans have been explained by fragmentation by plate tectonics of ancestral shallow water marine populations. The amphipod stygobiont genus *Pseudoniphargus* is distributed across the Mediterranean region but also in the North Atlantic archipelagos of Bermuda, Azores, Madeira and the Canaries. We used species delimitation methods and mitogenome phylogenetic analyses to clarify the species diversity and evolutionary relationships within the genus and timing their diversification. Analyses included samples from the Iberian Peninsula, northern Morocco, the Balearic, Canarian, Azores and Madeira archipelagoes plus Bermuda. In most instances, morphological and molecular-based species delimitation analyses yielded consistent results. Notwithstanding, in a few cases either incipient speciation with no involvement of detectable morphological divergence or species crypticism were the most plausible explanations for the disagreement found between morphological and molecular species delimitations. Phylogenetic analyses based on a robust calibrated mitochondrial tree suggested that *Pseudoniphargus* lineages have a younger age than for other thalassoid amphipods displaying a disjunct distribution embracing both sides of the Atlantic Ocean. A major split within the family was estimated to occur at the Paleocene, when a lineage from Northern Iberian Peninsula diverged from the rest of pseudoniphargids. Species diversification in the peri-Mediterranean area was deduced to occur in early Miocene to Tortonian times, while in the Atlantic islands it started in the Pliocene. Our results show that the current distribution pattern of *Pseudoniphargus* resulted from a complex admix of relatively ancient vicariance events and several episodes of long- distance dispersal.

1. Introduction

Cryptic lineage complexes, defined as groups of genetically distinct but morphologically similar or indistinguishable species, have been reported in many taxonomic groups and environments (Pfenninger and Schwenk, 2007). They are common among amphipod crustaceans, one of the most diverse and ecologically important groups of invertebrates in continental waters (Witt and Hebert, 2000; Witt et al., 2006; Fišer et al., 2018; Copilaş-Ciocianu et al., 2018). Here, the frequency of cryptic species is particularly high among obligate subterranean (stygobiont) forms, where the strong directional selection imposed by the extremely demanding habitat conditions favors the emergence of morphological convergence (Lefébure et al., 2006, 2007; Delić et al., 2017). In this regard, the shared loss or reduction of eyes and of body pigmentation, together with the elongation of appendages, are only the gross and more remarkable manifestations of this syndrome among cave amphipods (Barr and Holsinger, 1985).

Pseudoniphargus Chevreux, 1901 and the monotypic *Parapseudoniphargus* Notenboom, 1988 are the only members of the amphipod family Pseudoniphargidae Karaman, 1993. Pseudoniphargids are exclusively stygobiont and occur in a broad array of subterranean habitats, spanning from brackish-water coastal wells and caves to the hyporheic medium of mountain streams located up to 1420 m above sea level (Stock, 1980; Notenboom, 1987a). Despite none of its members has ever been recorded in ordinary marine habitats, the family is considered to be of marine (thalassoid) origin. This is based on (i) the presence of several species in transitional habitats with the sea, such as brackish-water anchialine caves or intertidal coastal springs (Stock, 1980; Stock et al., 1986; Stock and Abreu, 1992; Bréhier and Jaume, 2009); (ii) the occurrence of limnic species on islands never connected to continental landmasses; and (iii) the limitation of continental records of the family to occur only on areas formerly occupied by epicontinental seas (Notenboom, 1991).

Pseudoniphargus currently comprises 71 species (Horton et al., 2018), all showing an extremely localized distribution and often representing single-site endemics (Stock, 1980; Notenboom, 1986, 1987a, 1987b; Karaman and Ruffo, 1989; Jaume, 1991; Messouli et al., 2006; Bréhier and Jaume, 2009; Stokkan et al., 2018). The genus is present in

* Corresponding author.
E-mail address: jpons@imedea.uib-csic.es (J. Pons).

https://doi.org/10.1016/j.ympev.2018.07.002
Received 28 February 2018; Received in revised form 28 June 2018; Accepted 4 July 2018
Available online 10 July 2018
1055-7903/

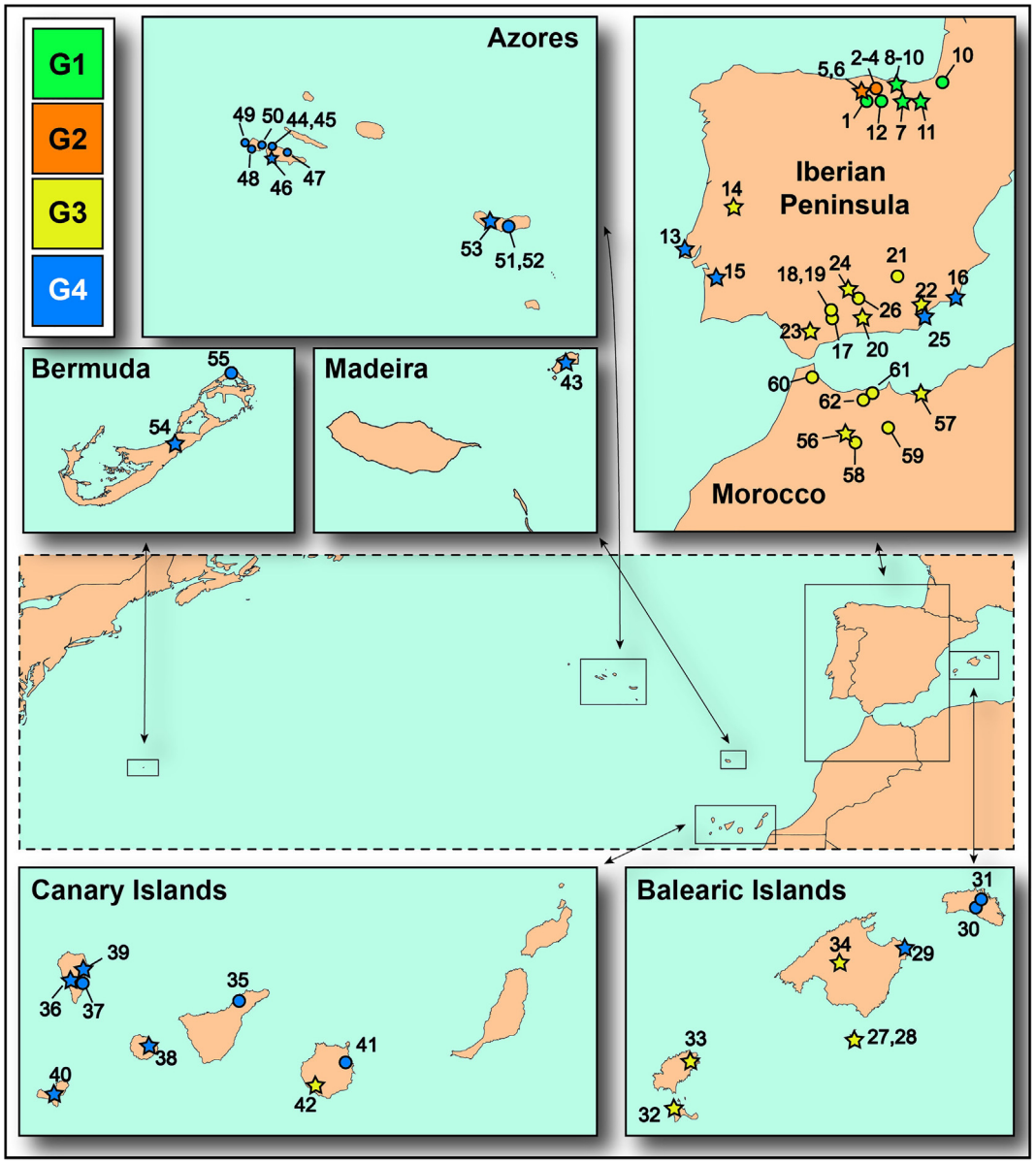

Fig. 1. Map showing approximate geographic locations for the *Pseudoniphargus* sampling sites. Circles show localities with taxa selected for mitogenome sequencing. See Supplementary Table S1 for the geographical details for each sample and species. *Pseudoniphargus* species were divided in four main groups G1-G4 based on phylogenetic results (see Figs. 2–4).

North Africa (Morocco and Algeria), the Mediterranean region –including most of its islands–, the Iberian Peninsula plus the North Atlantic archipelagos of Canaries, Madeira and Azores, whereas two species occur on Bermuda, on the west side of the mid-Atlantic rift (Stock et al., 1986). *Pseudoniphargus* is however absent from the American continent, in contrast to the distribution shown by other thalassoid stygobiont crustaceans such as *Metacrangonyx* amphipods or *Tethysbaena* thermosbaenaceans, present on both shores of the Atlantic (Jaume and Christenson, 2001; Wagner, 1994).

The occupation of inland subterranean waters by *Pseudoniphargus* is assumed to result from the stranding of populations of a marine ancestor after the withdrawal of the sea during periods of marine regression (Stock, 1977, 1980). This process led to the isolation of populations and their eventual speciation on the newly emerged land, to the point that the branching pattern within a determinate *Pseudoniphargus* lineage might be synchronous with the sequence of regression events through which the stygobionts became isolated from their marine ancestor (Stock, 1980; Notenboom, 1988, 1991).

Pseudoniphargus, as most stygobionts, have extremely reduced long-range dispersal due to intrinsic biological and ecological features. On one side, the lack of vision and of body pigmentation increases considerably their vulnerability to predation, competition or to damaging radiations in epigean habitats. Furthermore, as in the rest of amphipods and other groups such as the thermosbaenaceans, females brood embryos in a marsupium until they complete their development. No eggs or free-swimming larvae are released to the water column to be transported passively by sea currents, which is one of the ordinary ways through which aquatic invertebrates attain a trans-oceanic distribution. In these subterranean forms, dispersal is so reduced that there is virtually no gene flow between neighboring anchialine cave populations (Bauzà-Ribot et al., 2011; Cánovas et al., 2016).

Under these assumptions, the amphi-Atlantic distribution displayed by *Pseudoniphargus* and other thalassoid stygobionts is better explained in terms of vicariance rather than of dispersal. It has been proposed that their current distribution would be the outcome of the fragmentation by plate tectonics of ancient, ancestral shallow-water marine populations

(Stock, 1993; Wagner, 1994; Bauzà-Ribot et al., 2012; Jurado-Rivera et al., 2017). In this scenario, the presence of members of these genera on geologically young Atlantic oceanic islands could be explained if these islands had existed as shallow banks or seamounts since before the complete opening of the Atlantic Ocean, so that the ancestors of the recent species could remain associated with these marine shallow waters until the emergence of the islands (Fernández-Palacios et al., 2011; Bauzà-Ribot et al., 2012; Botello et al., 2013; Hou and Li, 2017).

The few cases in which this hypothesis has been tested using time-calibrated molecular phylogenetic methods have shown a relative congruence between genetic divergence and vicariance by plate tectonics. Thus, in metacrangonyctid amphipods, the major diversification episodes established in a dated robust phylogeny were compatible with a plate tectonics-driven, vicariant scenario (Bauzà-Ribot et al., 2012). But similar studies carried out on *Typhlatya* cave shrimps concluded that not only ancient vicariance, but also ancient long-distance dispersal could have contributed to their current distribution pattern (Botello et al., 2013; Jurado-Rivera et al., 2017).

Here we present a phylogenetic survey of *Pseudoniphargus* including representatives from all major geographical areas where the genus has been recorded. We use a large mitochondrial cytochrome oxidase subunit 1 (*cox1*) sequence dataset to explore species diversity under several species delimitation criteria and establish how widespread is crypticism among *Pseudoniphargus*. We select a set of key representative taxa among those resulting from the species delimitation analyses to build a robust phylogeny of the genus based on the complete set of protein-coding mitochondrial genes (mitogenomics). This phylogenetic hypothesis and an approximate time frame for species diversification are used to assess the potential roles played by both vicariance and long-distance dispersal in the biogeographic history of *Pseudoniphargus*.

2. Material and methods

2.1. Taxon sampling

We collected representatives of *Pseudoniphargus* from 62 localities (mostly wells and caves) distributed along the Iberian Peninsula, northern Morocco, the Balearic, Canarian, Azores and Madeira archipelagoes, plus Bermuda (Fig. 1; Supplementary Table S1). The dataset includes 30 out of the 71 species currently recognized in the genus, plus 17 presumed new species not yet formally described. Specimens were preserved in the field in 96% ethanol immediately after collection. Voucher specimens and DNA aliquots were deposited at IMEDEA (Spain). Most species were collected at single localities except for a few cases where the same species was recorded in multiple sites, viz. *P. brevipedunculatus* (ten localities on the Azores Islands), *P. elongatus* (five localities in N Spain), *P. mercadali* (three localities on the Balearic Islands) and *P. ruffoi* (three localities in Morocco). Two species appeared syntopically at seven sampling sites, viz. *P. triasi* and *P. daviui* on the same well at Cabrera (Balearic Islands), *P. carpalis* and *P. grandimanus* in Red Bay cave (Bermuda), whereas *P. longipes* and two cryptic species (*P.* sp6-Morocco A and B) were found sharing the same well at Sidi Abdellah (Taza; Morocco).

2.2. PCR amplification and sequencing of cox1 sequences

Genomic DNA was individually purified from whole specimens using the Qiagen DNeasy Blood & Tissue kit (Qiagen, Hilden, Germany) following the manufacturer's protocol. A total of 410 individuals were sequenced from 30 described species plus 17 recognized herein as potentially new (Supplementary Table S1). We aimed to sequence a minimum of five specimens per site whenever possible, but the actual number varied largely between one and 25 depending on sampling success (Supplementary Table S1). Taxa were identified based on their original descriptions (Bréhier and Jaume, 2009, and references therein; Messouli et al., 2006; Stokkan et al., 2018). PCR amplification of mitochondrial cytochrome *c* oxidase subunit 1 (*cox1*) was performed mainly using the primer-pair LCO/HCO (Folmer et al., 1994), but in some cases we used an internal degenerated primer set especially designed for this genus (amplicon of 463 bp), based on the sequences amplified with the previous primers (PSNI_cox1_F_A39 5′-GCTCATGC-TTTTGTTATGATTTTYTTYATRGT-3′ and PSNI_cox1_R_A71 5′-CAAAA-CAGATGTTGATAAAGAATTGGRTCNCCNCC-3′; Stokkan et al., 2016). PCR and Sanger sequencing followed protocols described elsewhere (Bauzà-Ribot et al., 2011). DNA sequences were edited in CodonCode Aligner v5.1.5 (CodonCode Corporation, Denham, MA, USA) and aligned using MAFFT (Katoh, 2013).

2.3. Single locus species delimitation analyses

Two tree-based and one distance species delimitation methods were explored. First, we applied the Generalized Mixed Yule Coalescent model (GMYC; Pons et al., 2006; Fujisawa and Barraclough, 2013). This method estimates species boundaries implementing a likelihood ratio test to compare the null model assuming a single coalescent branching rate across a clock-like tree with a complex model including both coalescent and Yule branching models. The R library SPLITS v1.0-19 (Ezard and Fujisawa, 2009) was used in this analysis specifying a single threshold as recommended by Fujisawa and Barraclough (2013) on an ultrametric tree estimated with BEAST v1.8.2 (Drummond and Rambaut, 2007). The GMYC support value of each node representing a transition from species to population was calculated as the sum of Akaike weights of candidate delimitation models where the node is included (Fujisawa and Barraclough, 2013). This allows assessing whether the branch leading to a node contains a coalescence-to- speciation threshold under different coalescent models (Fujisawa and Barraclough, 2013). A node support value of 1 means that all coalescent models tested support the existence of a speciation event on that branch, while lower values indicate that fewer coalescent models support a particular speciation event. We set an arbitrary minimum value of 0.9 to consider a GMYC entity as supported by most coalescent models. To perform the analysis, 1st plus 2nd codon positions and 3rd positions were considered as separated partitions due to their marked differences in nucleotide composition and substitution rates (Stokkan et al., 2016). Models of nucleotide substitution were evaluated with MrAIC.pl v1.4.6 (Nylander, 2004) yielding TRN + G and HKY + G as best-fitting models for 1st + 2nd and 3rd codons positions, respectively. The analysis implemented a coalescent constant population size as tree model and a single uncorrelated relaxed clock with a log-normal distribution. Substitution rate was arbitrarily set with a mean of the standard 0.0115 nucleotide substitutions per site and lineage per million years [log mean −4.465, stdev 0.1, 95% confidence interval 0.0095–0.014] to optimize the threshold (Brower, 1994). Runs convergence was assessed in Tracer v1.6 (Rambaut et al., 2015) with a 10% burnin. Species boundaries and their support were also estimated under Poisson Tree Processes (PTP; Zhang et al., 2013) using a single threshold under a Maximum Likelihood (ML) criterion as implemented in the python version of PTP v2.2 (Zhang et al., 2013). Trees were estimated in RAxML v8.2.4 (Stamatakis et al., 2006) implementing the same two partitions as above and a GTR + CAT model for each independent partition. One-thousand tree topologies incorporating branch lengths were estimated using the fast bootstrap algorithm.

Additionally, species were delimited using genetic distances in Automatic Barcode Gap Discovery (ABGD; Puillandre et al., 2012). This approach finds recursively the slope above a cut-off value (X) that splits the data in intra- and interspecific distances starting from an arbitrary minimum (p) and maximum (P) value. We implemented a p value of 0.0001 enabling the existence of nearly identical haplotypes, and a P value of 0.1, after the maximum intraspecific distance found in *Metacrangonyx longipes* Chevreux, 1909, a stygobiont amphipod species densely sampled in the Balearic Islands (Bauzà-Ribot et al., 2011). Distances were calculated using the Tamura-Nei nucleotide substitution

model, implemented in this case with a lower cut-off value (X = 1.0) since the default slope threshold (X = 1.5) was not significant and produced a single species. These values were used to estimate the inflection point between two distributions of ranked frequencies of pairwise distances using ten recursive steps, i.e. the minimum optimal gap between intra- and interspecific distances.

2.4. Mitochondrial genome sequences

The complete or almost complete DNA sequences for mitogenomes of 28 *Pseudoniphargus* putative species out of a total of 47 were obtained using any of these three different methods: (i) long PCR mitochondrial fragments sequenced in a Roche GS FLX or GS Junior platform (eight species) as in Bauzà-Ribot et al. (2012); (ii) sequencing the whole genome at low coverage in Illumina platforms (18 species) (see methods in Pons et al., 2014; and Stokkan et al., 2016); and (iii) in cases of low genomic DNA yield, the mitogenome was amplified by multiple displacement amplification using specifically designed primers followed by sequencing in an Illumina platform (four species) (Blanco et al., 1989) (see Supplementary Methods). Indexed libraries were quantified by qPCR, pooled in equimolar concentration, and paired-end sequenced in a Miseq v2 (2 × 150) or one lane using HiSeq2500 (2 × 150 or 2 × 160 reads). Fastq files were generated and demultiplexed with bcl2fastq software (Illumina) and adapters and low-quality bases removed from reads using Trimmomatic v0.33 (Bolger et al., 2014). Contigs were assembled *de novo* with Trinity v2014-04-13p1 (Grabherr et al., 2011), and Ray v2.3.1 (Boisvert et al., 2010) using collapsed and truncated paired- end reads only. Mitogenome contigs were annotated in MITOS webserver (Bernt et al., 2013). Start and stop codon regions of protein-coding genes (PCGs) and the 5′ and 3′ ends of ribosomal genes were refined manually by comparing them to sequences available on databases. Secondary structures of tRNAs were corroborated with tRNAscan-SE (Schattner et al., 2005).

2.5. Mitochondrial phylogenetic analyses

We included the mitochondrial PCG sequences of 19 outgroup taxa taken from the GenBank and metAMiGA databases to root the *Pseudoniphargus* tree (Feijão et al., 2006): one mysid, eight isopods and ten amphipods (see Supplementary Table S2). The newly obtained *Pseudoniphargus* mitochondrial genome sequences were first translated to protein, aligned with Muscle v3.8.31 (Edgar, 2004) with default parameters and back-translated to nucleotides conserving the integrity of codon triplets but excluding terminal stop codons. The mitogenomes of three species reported elsewhere (*Pseudoniphargus sorbasiensis* LN871175; *P. gorbeanus* LN871176 and *P. daviui* FR872383) were included in the analyses (Stokkan et al., 2016). Regions aligned ambiguously, in particular at 5′ and 3′ sequence ends due to uneven sequence lengths were removed as codons with Gbloks v0.91b (Castresana, 2000) under relaxed conditions. After trimming, most of the 13 mitochondrial PCGs retained more than 94% of the original positions of the alignment except the genes nad4L (91.26%), nad2 (90.57%), nad6 (85.41%), and the highly variable atp8 (74.55%).

Phylogenetic trees were built under a maximum likelihood framework using both DNA and protein datasets in IQ-TREE (Nguyen et al., 2015), with the best partition scheme and models estimated in PartitionFinder (Lanfear et al., 2012) and branch lengths calculated independently for each partition (i.e. unlinked branch lengths). Tree topologies were also assessed under parsimony criterion in PAUP v4.0 beta 10 with 1000 random addition replicates, saving 50 trees per replicate, and heuristic searches with tree-bisection-reconnection branch-swapping (Swofford, 2002). Node support was assessed by 1000 bootstrap replicates in ML and parsimony. Tree searches were also performed under the Bayesian criterion in PhyloBayes mpi v1.5a implementing the GTR + CAT model, as this model has been shown to be less prone to phylogenetic errors caused by compositional bias or saturation (Lartillot and Philippe, 2004; Lartillot et al., 2009). Two independent runs were sampled every 1000 generations until convergence was reached. To assess nucleotide substitution saturation, the Xia saturation test was implemented using the whole dataset and for first, second and third codon sites separately as implemented in DAMBE v6.0.0 (Xia and Lemey, 2009; Xia et al., 2003). Saturation was also explored plotting corrected and uncorrected branch lengths estimated under a fixed topology in IQ-TREE. Correlation between patristic distances was estimated with the software Patristic (Fourment and Gibbs, 2006).

2.6. Calibration of the molecular clock and dating

There are no fossils of *Pseudoniphargus* known, and the amphipod fossil record is not older than Eocene in age (niphargids and crangonyctids preserved in Baltic amber 54–40 million years in age; Jażdżewski et al., 2014; Starr et al., 2016). For that reason, we relied on palaeogeographical evidence to constraint the age of a set of nodes in our *Pseudoniphargus* tree. Specifically, the geological age of oceanic islands or the age of emergence from the sea of continental areas where sister species occur were assumed to precede the divergence of sister taxa on those areas. The ages of the three geological events related to the diversification of particular *Pseudoniphargus* lineages were considered as soft constraints with a parametric log-normal distribution that assigns non-zero probabilities to all possible age values. The midpoint of the extent of each geological event was arbitrarily considered as the age with the highest probability in the distribution. Congruence among calibration points was explored performing a cross-validation analysis, i.e. comparing three additional BEAST runs, each calibrated with a single geological event. The geological events used for this purpose in our analysis were: (i) The emergence of the Basque Country (western edge of the Pyrenees; northern Spain) at the Early Oligocene (33.7 Ma; Rögl, 1998). There, a triplet of sister species occurs (*P. gorbeanus/P. unisexualis/P.* sp1-Basque). Assuming that the divergence of these three species from a common marine ancestor was driven by past episodes of sea level regression (Stock, 1980; Notenboom, 1991; Boutin and Coineau, 1990), it could not have happened before the first subaerial exposure of that area. We constrained this node with a strong prior by implementing a log-normal distribution with a mean (M) of 32.7 Ma and standard deviation (SD) of 0.1 (95% confidence interval 26.8–39.6). (ii) The establishment of the so-called Southern Riffian Corridor across northern Morocco between 8 and 6.1 Ma (Achalhi et al., 2016). This gateway enabled the temporary direct connection between the Mediterranean and the Atlantic Ocean up to the closing of the Strait of Taza during the Messinian. The sister species *P. ruffoi/P. longipes* are found one at each side of this vanished sea corridor. As in the preceding case, we consider that the origin of these two species cannot be older than that age, assuming they derive from a common marine ancestor. We defined a normal distribution as a soft constraint for this node with M = 7.1 Ma and SD of 0.1 (5.8–8.5). (iii) The emergence of La Palma (Canary Islands), which harbors the sister species *P. cupicola/P. multidens*. The age of the split between these two taxa cannot be older than the first subaerial exposure of the island (ca. 2.0 Ma; Carracedo et al., 2001). We defined a log-normally distributed function as a soft constraint for this node with M = 2.0 Ma and SD of 0.1 (1.6–2.4).

For the calibration analyses we excluded outgroups and rooted the trees according to the topologies obtained in the analyses including outgroups. Tree topologies, model parameter values and node ages were co-estimated and optimized in Beast v1.8.2 implementing the best partition scheme and models described above. Bayesian analyses were run for 150 million generations. Convergence of the run was assessed in Tracer v1.6 (Rambaut et al., 2015) ensuring parameter values to have ESS values > 200. Mean values and confidence intervals of the parameters and ages were estimated in TreeAnnotator after a burnin of the first 15 million generations. We implemented default priors for all parameters except for clock and Yule rate priors since the ones by

default did not converged during path sampling. The substitution rate prior (ucld.mean) for 1st codon sites was set as a log normal distribution in real space with M = 0.005 and SD = 1.5 (95% confidence interval $8.58 \times 10e^{-05}$–$3.07 \times 10e^{-02}$); M = 0.1 and SD = 1.5 ($1.72 \times 10e^{-04}$–$6.14 \times 10e^{-02}$) for 2nd codon positions; and M = 0.5 and SD = 1.0 ($4.27 \times 10^{e-3}$–0.21) for 3rd codon sites and as global rate. The tree prior for Yule birth rate parameter was also set to a log-normal distribution in real space with M = 0.5 and SD = 3.0 (95% confidence interval $1.55 \times 10e^{-05}$–1.98). We estimated node ages under a strict clock, and two types of relaxed clocks where rates on descendant branches are independent of the rate at the parent branch: uncorrelated log-normal clock (UCLN) and random local clocks (RLC). Runs implementing RLC were run for 500 million generations since it took about 280 million generations until convergence, which were discarded as burnin. Different partition schemes and clocks were compared based on Bayes Factors estimated by marginal likelihoods using path sampling and the stepping stone model as implemented in Beast. We performed 100 steps of 5 million generations each using a path scheme with a betaQuantile 0.33 (Baele et al., 2012), discarding 25% of the run as burnin.

3. Results

3.1. Phylogeny and species delimitation based on cox 1 sequences

The mitochondrial *cox1* sequences obtained from 410 *Pseudoniphargus* individuals showed no indels, stop codons or singleton non-synonymous substitutions, suggesting the absence of nuclear mitochondrial DNA segments in the dataset (accession numbers LS482437-LS482846). Invariant and parsimony-informative nucleotide positions accounted for 53.3% and 43.7%, respectively. Only two localities placed in close proximity on the island of Cabrera (Balearic Islands), where *P. daviui* occur, and two wells harboring *P. brevipedunculatus* on Pico Island (Azores) showed shared haplotypes, while all other collecting sites rendered locality-specific mitochondrial sequences. After collapsing into identical sequences, a total of 182 haplotypes were retained. Bayesian and ML phylogenetic trees showed four major clades, with weakly supported relationships among them (Fig. 2):

(i) Clade G1, including exclusively species from northern Spain, from the upper reaches of the Ebro river basin and valleys and massifs of the Basque Country; (ii) Clade G2, comprising a single species from the Cantabrian mountains in northern Spain. (iii) Clade G3, a mostly Mediterranean clade embracing species from S and SE Spain, Portugal, the Balearic Islands and northern Morocco, but also including a species from Gran Canaria (*P.* sp2-Canaries); and (iv) clade G4, included most of the species from Atlantic Islands (Canaries, Madeira, Azores, Bermuda) but also several taxa from the Balearics, Portugal and SE Spain.

The GMYC algorithm applied to the ultrametric tree favored a two-parameter model including both coalescent and Yule branching over the null model with a single coalescent parameter ($P < 1e^{-15}$). The single threshold approach retrieved 63 entities defined herein as Molecular Operational Taxonomic Units (MOTUs), with a confidence interval ranging from 59 to 67 (Table 1; Fig. 2). Twenty-one of these MOTUs were represented each by single specimens, whereas the remaining 42 MOTUs embraced multiple individuals (Fig. 2). Thirty of the GMYC groupings found were consistent with known species, whereas other 17 were previously recognized based on the morphological analyses herein undertaken (considered here as undescribed morphotypes). Most of the MOTUs had a high GMYC support (i.e. most of the coalescent models tested validate them), with values ranging between 0.9 and 1.0, with the exception of the groupings identified within *P. brevipedunculatus*, *P. elongatus*, *P. gorbeanus*, *P. longipes* and *P.* sp1-Andalusia and *P.* sp3-Andalusia (see Fig. 2 and Supplementary Fig. S1 for precise values).

The PTP method discriminated among 55 MOTUs, 44 of which were consistent with those recognized by GMYC (Table 1; Fig. 2). This method in turn rendered a slightly better correspondence between morphologically defined species and MOTUs than the GMYC. Thus, PTP and morphology confirmed the same species for *P.* sp1- Andalucia, *P.* sp3-Andalusia, *P. brevipedunculatus* and *P. cupicola*. On the contrary, PTP split *P. gorbeanus* in one more group than GMYC but merged the sequences of *P. guernicae* and *P.* sp1-Basque, two species recognized both morphologically and by GMYC, in a single entity.

The distance-based method ABGD estimated the maximal intraspecific distance to be P = 4.64%, retrieving a total of 49 MOTUs

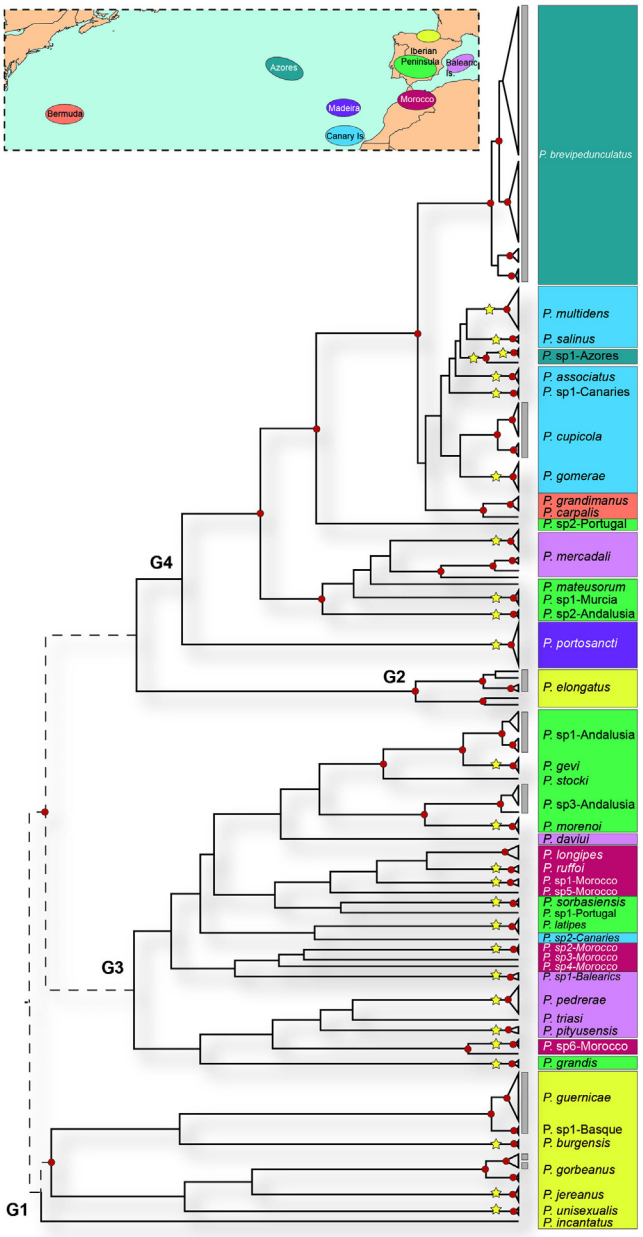

Fig. 2. Summary of tree-based species delimitation results for GMYC and PTP algorithms shown on a *cox1* Bayesian phylogenetic tree. Each tree terminal (branch or triangle) summarizes a GMYC entity, with triangles merging the different haplotypes corresponding to the same MOTU. Vertical grey bars indicate PTP MOTUs that differ from GMYC results. Red dots on nodes denote a Bayesian posterior credibility support value higher than 0.95. Putative species highly supported by both GMYC and PTP analyses (≥90%) are indicated by yellow stars (see Supplementary Fig. S2 for more details). Branches with dotted lines are not in scale and were trimmed as to fit the figure in a single page. G1-G4 indicate the four main groups found in the *Pseudoniphargus* species studied.

Table 1
Comparison of the taxonomically recognized and newly proposed species of *Pseudoniphargus* based on morphology with the molecular operational taxonomic units (MOTUs) estimated herein by three species delimitation methods. Numbers in brackets indicate number of MOTUs recognized when considering GMYC and PTP support values (nodes supported by more than 90% of coalescent models in GMYC or tree-topologies in PTP; see Material and Methods and Fig. 2). A 0.5 value indicates that two sister species were merged together in a single unit by a particular method. Asterisks denote cases where delimitation was based on a single specimen or *cox1* haplotype sequence. Table also includes number of individuals sampled per taxonomic (# ind) species and their intraspecific divergence (p-distance) based on *cox1* sequence (p-dist).

Species	# ind	p-dist	GMYC	PTP	ABGD
P. burgensis	2	0.000	1	1	1
P. elongatus	10	0.046	5(4)	3(2)	2
P. gorbeanus	22	0.013	2(2)	3(1)	1
P. guernicae	14	0.008	1	0.5	0.5
P. incantatus	2	0.000	1	1	1
P. jereanus	6	0.001	1	1	1
P. unisexualis	5	0.001	1	1	1
P. sp1-Basque	4	0.001	1	0.5	0.5
P. gevi	7	0.001	1	1	1
P. grandis	4	0.003	1	1	1
P. latipes	8	0.002	1	1	1
P. morenoi	6	0.001	1	1	1
P. sorbasiensis	11	0.000	1	1	1
P. stocki	3	0.000	1	1	1
P. sp1-Andalusia	11	0.013	2(1)	1	1
P. sp2-Andalusia	5	0.001	1	1	1
P. sp3-Andalusia	5	0.010	2(1)	1	1
P. sp1-Murcia	3	0.003	1	1	1
*P. mateusorum**	1	n/a	1	1	1
P. sp1-Portugal*	1	n/a	1	1	1
P. sp2-Portugal	4	0.000	1	1	1
P. daviui	19	0.001	1	1	1
P. mercadali	18	0.073	4(2)	4(2)	3
P. pedrerae	12	0.007	1	1	1
P. pityusensis	5	0.009	1	1	1
P. triasi	2	0.000	1	1	1
P. sp1-Balearics	8	0.003	1	1	1
P. associatus	7	0.001	1	1	1
P. cupicola	26	0.013	2(2)	1	1
P. gomerae	25	0.001	1	1	1
P. multidens	22	0.004	1	1	1
P. salinus	7	0.001	1	1	1
P. sp1-Canaries	4	0.000	1	1	1
P. sp2-Canaries*	2	0.000	1	1	1
P. brevipedunculatus	60	0.018	4(3)	1	1
P. sp1-Azores	7	0.014	2(1)	2(1)	1
P. portosancti	11	0.002	1	1	1
P. carpalis	4	0.000	1	1	0.5
P. grandimanus	3	0.009	1	1	0.5
P. longipes	14	0.004	1	1	1
P. ruffoi	5	0.003	1	1	1
P. sp1-Morocco	3	0.007	1	1	1
P. sp2-Morocco	3	0.000	1	1	1
P. sp3-Morocco*	1	n/a	1	1	1
P. sp4-Morocco*	1	n/a	1	1	1
P. sp5-Morocco*	1	n/a	1	1	1
P. sp6-Morocco	6	0.038	2(2)	2(2)	2

(Table 1). Forty out of the 47 morphologically recognized species corresponded to a single entity in this analysis, except for *P. grandimanus* and *P. carpalis*, that were merged into one, as it was the case for *P. guernicae* and *P.* sp1-Basque. *Pseudoniphargus mercadali* was split into three entities using ABGD, whereas *P.* sp6-Morocco and *P. elongatus* were split each into two.

In summary, species coincidentally detected by diagnostic morphological features and three molecular species delimitation methods accounted for ca. 80% of the cases (38 species) (Table 1). In six other cases (13%), the discrepancy found between the morphological classification and one of the three delimitation methods might suggest we are in front of transition events from populations to species (incipient speciation) but where the morphologies of descendants have not diverged yet. Finally, in three assignments (7%), genetic lineages appear to be relatively old phylogenetically, but have proven to be undistinguishable morphologically and should be considered as true cryptic species (between two and four phyletic lineages present in *P. mercadali* and *P. elongatus*, and two in *P.* sp6-Morocco (Table 1).

3.2. Mitochondrial genomes

Specimens representative of 28 MOTUs were selected for sequencing their mitochondrial genome and study of their phylogenetic relationships, assuring an even sampling of all *Pseudoniphargus* distributional areas. Three additional MOTUs represented by the mitogenomes of other *Pseudoniphargus* species obtained previously were also included in the analyses (Stokkan et al., 2016). The mitogenome sequence coverage obtained was dependent of the amplification and sequencing methods used but was generally higher than 50x (Table 2; Supplementary Methods). In two species, *Pseudoniphargus* sp2-Portugal and *P. salinus*, the PCG sequences were incomplete as only two non-overlapping fragments were obtained probably due to technical difficulties in sequencing long polyA/T runs. In addition, the analysis of the mitogenome sequences obtained from pooled individuals of *P.* sp6-Morocco showed the presence of two divergent mitogenomes (divergence $> 10\%$), confirming the presence of two syntopic cryptic species in their sampling locality.

The 29 newly obtained mitogenomes showed the 37 genes characteristic of metazoans: 13 PCGs, 22 tRNA genes, plus two rRNA genes with a length ranging 14–15 kb. Gene arrangement was not conserved across species as described previously (Stokkan et al., 2016). In addition to the three gene orders already described in the latter paper, two of them involving shifts of protein-coding genes, another two gene arrangements affecting the position of several tRNA genes were found in the sampled species (not shown).

3.3. Mitochondrial genome phylogeny

The individual alignments of the 13 PCGs of the *Pseudoniphargus* species plus outgroups after excluding ambiguous positions were concatenated in a single dataset of 10,833 bp (corresponding to 3611 amino acids). Sequences showed a high A + T nucleotide bias, especially at third codon positions, as is usually the case for arthropod mitochondrial DNA (Hassanin, 2006; Stokkan et al., 2016). Xia's test showed relatively low levels of nucleotide substitution saturation under the assumption of a symmetric tree even using outgroup sequences ($p < 0.001$) and all codon positions. Low to moderate saturation was also found at 1st and 2nd codon positions (0.3 and 0.4, compared to a critical value of 0.8). A higher, but still non-critical value was recovered for 3rd codon positions (0.79 vs. 0.83). This was confirmed by plotting branch lengths estimated under the simple F81 + G substitution model versus the complex GTR + G (Supplementary Fig. S2). After refining the results obtained in PartionFinder using Bayesian Information Scores (BIC), the best partition consisted of subdividing the nucleotide dataset in four partitions: 1st codon positions; 2nd codon positions; 3rd codon positions coded on the + strand and 3rd codon positions coded on the – strand (the genes *nad1, nad4, nad4L, nad5*) (Table 3), while the best substitution model for each partition consisted on GTR + G.

The ML phylogenetic tree including outgroups retrieved two main *Pseudoniphargus* mitogenome lineages, of which one appears subdivided in turn into another three clades (Fig. 3), in accordance with the *cox1* phylogeny (Fig. 2). The major clade, coincident with *cox1* species-group G1, comprises exclusively the three taxa occurring around the Gulf of Biscay in northern Spain *(Pseudoniphargus gorbeanus, P. unisexualis* and *P. sp1*-Basque). The second major clade includes all the remaining sampled species of the genus (Fig. 3). This clade can be further subdivided into clade G2, including only the species *P. elongatus*, which is distributed throughout Santander and the north of Burgos provinces in

Table 2
List of the *Pseudoniphargus* species whose mitogenome sequences were obtained in the present study. GenBank accession numbers and sampling locality are indicated, as are details on the sequencing method used (SM), sequence length, number of reads (x10^3), coverage depth and average length of mapped reads in bp. Sequencing methods are as follows: 1) Long PCR Fragments and GS FLX or GS JUNIOR sequencing, 2) Whole genome sequencing at low coverage in Illumina platforms with individually tagged libraries (Miseq 2x150 bp, Hiseq2500 2x150 bp or 2x160 bp, and 3) Multiple displacement amplification and Miseq 2x150 bp without tagging. Details of the mitogenomes of three *Pseudoniphargus* species previously obtained by Stokkan et al. (2016) are indicated with an asterisk. The present study also obtained the mitogenome sequence of the outgroup species *Metacrangonyx dhofarensis*.

Species name	Locality	Genbank	SM	length	n reads	Coverage	Av. read
P. daviui *	Balearic Is.; Cabrera: Font de s'hort de Ca'n Feliu	FR872383	1	15,155	N/A	73	410
P. carpalis	Bermuda; Red Bay Cave	MH592150	1	14,861	15	258	522
P. gomerae	Canary Is.; La Gomera: well at Playa del Avalo (San Sebastián)	MH592127	1	14,152	21	136	246
P. cupicola	Canary Is.; La Palma: Charco Verde (Puerto Naos)	MH592125	1	15,351	18	196	268
P. multidens	Canary Is.; La Palma: well at Santa Cruz	MH592133	1	14,393	27	206	354
P. portosancti	Madeira; Porto Santo: Fonte do Tanque	MH592136	1	14,093	20	99	526
P. stocki	Spain; Cádiz: El Pozo Blanco well (Villaluenga del Rosario)	MH592152	1	14,697	12	364	381
P. gorbeanus *	Spain; Cigoitia (Alava): Artzegi'ko Koba	LN871176	1	14,190	29	148	481
P. unisexualis	Spain; Guipúzcoa: Zegama, Túnel de San Adrián	MH592147	1	14,969	16	181	412
P. grandis	Spain; Málaga: Fuente de la Fájara (Canillas de Aceituno)	MH592128	1	14,800	23	247	397
P. sorbasiensis *	Spain; Sorbas (Almería): Cueva del Agua	LN871175	1	15,460	22	271	401
P. brevipedunculatus	Azores; Pico: Calhau	MH592123	2	14,424	2,710	110	147
P. sp1-Azores	Azores; Sao Miguel: Sao Roque	MH592148	2	14,981	2,480	185	144
P. triasi	Balearic Is.; Cabrera: Font de s'hort de Ca'n Feliu	MH592146	2	15,109	2,940	419	148
P. pityusiensis	Balearic Is.; Ibiza: well at Sant Joan de Llabritja	MH592135	2	14,748	2,690	495	148
P. mercadali	Balearic Is.; Mallorca: Cova de na Barxa (Capdepera)	MH592131	2	14,402	4,510	53	138
P. sp1-Balearics	Balearic Is.; Mallorca: well at Mr. Toni Martínez House (Cas Canar)	MH592138	2	15,256	2,020	83	152
P. salinus	Canary Is.; El Hierro: Pozo de Las Calcosas	MH592149	2	9,801 + 3,760	2,610	17	150
P. ruffoi	Morocco; Berkane: Grotte de Chameau	MH592137	2	14,055	2,380	8	134
P. longipes	Morocco; Taza: well at Sidi Abdellah	MH592129	2	14,658	2,480	23	152
P. sp6-Morocco A	Morocco; Taza: well at Sidi Abdellah	MH592144	2	14,180	2,240	275	138
P. sp6-Morocco B	Morocco; Taza: well at Sidi Abdellah	MH592145	2	12,660	2,240	253	128
M. dhofarensis	Oman: well at Salalah	MH592124	2	14,399	3,490	35	152
P. sp1-Portugal	Portugal; Sicó: Gruta de Legaçao	MH592151	2	15,728	2,850	890	148
P. sp2-Portugal	Portugal; Sintra: Gruta de Assafora	MH592143	2	14,150	2,360	97	141
P. elongatus	Spain; Burgos: Cueva de Imunía (Portillo de la Sía)	MH592126	2	15,145	3,330	212	146
P. morenoi	Spain; Córdoba: Cueva del Yeso (Baena)	MH592132	2	14,810	2,710	112	145
P. sp1-Murcia	Spain; Murcia: Cueva del Agua (Isla Plana)	MH592140	2	14,170	230	156	149
P. sp2-Andalusia	Spain; Níjar (Almería): Pozo de los Frailes	MH592141	2	14,191	1,930	74	147
P. pedreae	Balearic Is.; Formentera: Coves de sa Pedrera (St. Fernando)	MH592134	3	14,740	1.1	32	152
P. sp2-Canaries	Canary Is.; Gran Canaria: Mina Los Roques (Barranco de Arguineguín; El Sao)	MH592142	3	15,380	1	476	152
P. mateosorum	Portugal; Lapa dos Morcegos	MH592130	3	14,939	1	114	152
P. sp1-Basque	Spain; Vizcaya: Cueva de San Pedro (Axpe; Busturia)	MH592139	3	14,187	0.98	1005	152

northern Spain, and clade G3, composed of a group of species from Morocco, the Balearic Islands, SW and SE Iberian Peninsula plus the new species *P.*sp2-Canaries from Gran Canaria (Canary Islands). Finally, clade G4 shows a surprisingly large geographic distribution including Madeira (*P. portosancti*), Mallorca in the Balearics (*P. mercadali*), the south of the Iberian Peninsula (4 spp.), and also Bermuda (*P. carpalis*), Azores (2 spp.), and the Canary Islands of La Gomera (*P. gomerae*), La Palma (2 spp.) and El Hierro (*P. salinus*).

Table 3
Comparison of different partition schemes based on Bayesian information Criterion (BIC = −2Ln + Kln(n), where Ln is the tree Likelihood, K the number of free parameters of the models including the number of branches per partition, and n the number of sites (10833 pb per nucleotide sequences, and 3611 characters per amino-acid and codon models). Tree length (TL) and increment of BIC values relative to the best partition scheme found in Partition Finder are also indicated (% Δ BIC). The best model for all partitions was GTR + G with 4 categories to estimate the alpha parameter. # The best partition scheme found by Partition Finder included third codon positions of *atp8* gene within first codon sites partitions. * The best partition scheme for amino-acid sequences in Partition Finder was partition one composed of *atp6*, *cox1*, *cox2*, *cox3*, *nad1* genes and the model mtART + F + I + G and partition 2 with *atp8*, *coob*, *nad2*, *nad3*, *nad4*, *nad5*, *nad6*, *nad4l* genes and the model JTT + F + I + G. Plus and minus refers on which strand are genes coded. The abbreviation GY indicate the Goldman and Young codon model.

Partition	Ln	TL	K	n partitions	BIC	% Δ BIC
Nucleotide models						
Partition Finder Best #	−326434.277	36.724	432	4	656881.987	0.000
Codon1,codon2,codon3plus,codon3minus	−326362.065	36.936	432	4	656737.561	−0.022
Codon1,codon2,codon3	−327496.221	31.639	324	3	658002.517	0.171
Codon1&codon2,codon3	−329269.870	31.654	216	2	660546.456	0.558
Bygene & bycodon	−322049.672	42.583	4212	39	683230.307	4.011
Bygene & bycodon (HKY + G)	−323077.401	42.482	4056	39	683836.470	4.103
Bygene	−331861.427	32.601	1404	13	676766.508	3.027
Single	−335344.159	25.314	108	1	671691.677	2.255
Codon Model						
Codon GY(HKY) + F3X4 + G	−324804.524	244.292	111	1	650518.330	NA
Aminoacid models						
Partition finder best*	−141189.818	20.615	238	2	284329.270	0.000
Single mtART + F + G	−142123.033	27.136	119	1	285220.882	0.314
Single mtZOA + F + I + G	−141325.081	23.948	120	1	283633.171	−0.245
Genes plus, Genes minus (mtZOA + F + I + G)	−140867.106	23.931	240	2	283700.230	−0.221

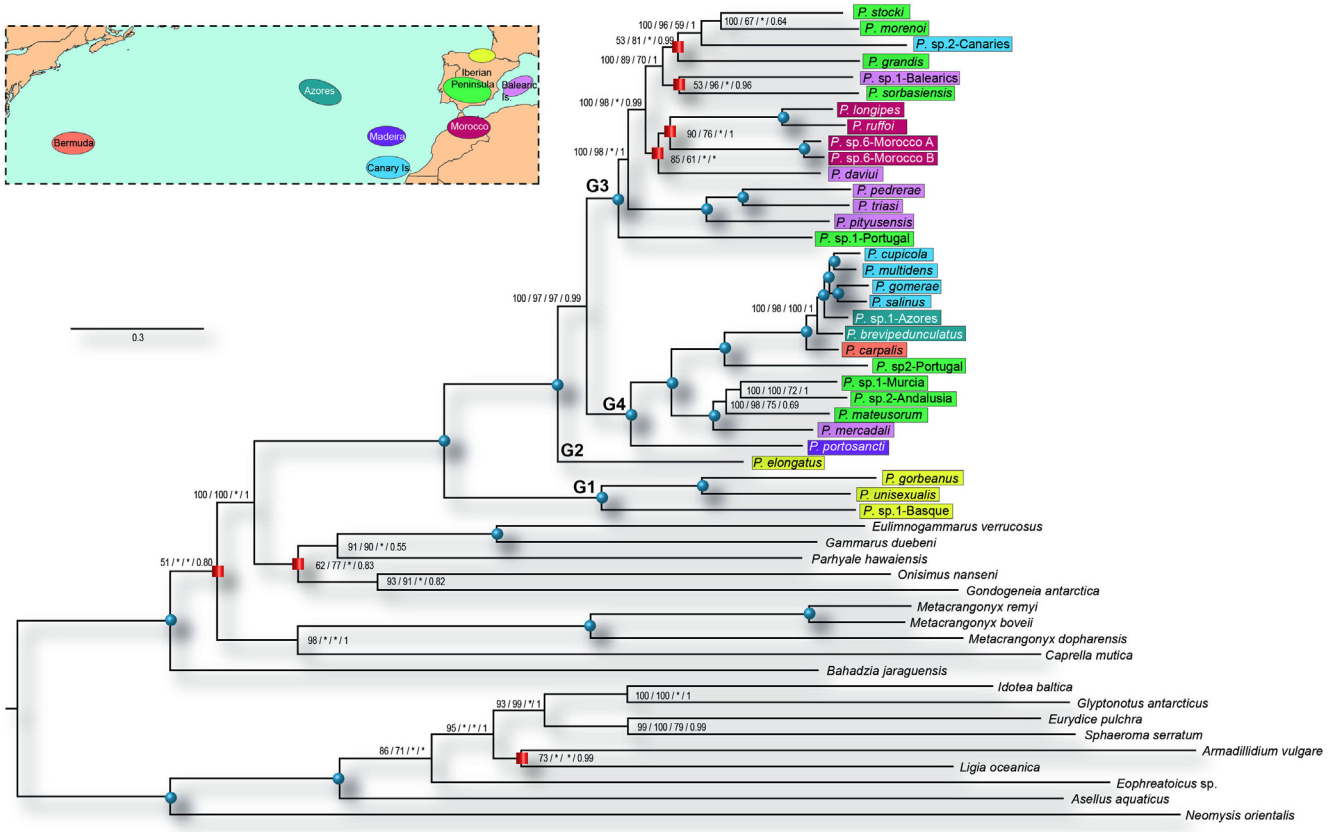

Fig. 3. Maximum Likelihood tree based on the nucleotide sequences of the 13 mitochondrial protein coding genes implementing the selected partitioning scheme (see text for details). Numbers on nodes indicate support values for (1) the best partition scheme, (2) codon GY model, (3) parsimony and, (4) Bayesian with GTR + CAT model. Nodes with full support for all methods are marked with blue dots. Red dots show nodes that were recovered in 60–85% of the ML analyses implementing different partition schemes (see Table 3). G1-G4 indicate the four main groups found in the *Pseudoniphargus* species studied.

The other partitioning strategies analyzed using the nucleotide sequence dataset resulted in identical or nearly identical topologies showing high support values for most nodes except for of the relationships among some of the taxa within clade G3 (Fig. 3). Similar results were obtained using parsimony, treating data as 62 different codon categories (GY98) and implementing the CAT model (Fig. 3) or using protein sequences analyzed by different methods and substitution models (Supplementary Fig. S3).

3.4. Calibration of molecular clock and dating

The best fitting clock model resulted from setting three independent uncorrelated log- normal clocks (1st codon, 2nd codon, 3rd codon), since third codon positions were considered a single partition in despite of the coding strand, and a Yule diversification model (Table 4). The chronogram of *Pseudoniphargus* diversification obtained after using the age of three geological events as node constraints to calibrate the tree (see Material and Methods) is shown in Fig. 4. The root of the tree, corresponding to the initial diversification of the sampled *Pseudoniphargus* taxa was estimated to fall in the Eocene, about 52.8 Ma (HPD95% = 46.5–59.5), while subsequent major splits took place at the early Oligocene (ca. 32 Ma; HPD95% = 27.5–36.4 Clades G2-G4 in Fig. 4), or during the Miocene (24.6 and 22.5 Ma for clades G3 and G4, respectively). Splits leading to the oceanic island species present on the Canaries, Azores and Bermuda occurred in the transition from the Miocene to the Pliocene (ca. 5 Ma, Fig. 4). Other partition schemes and the use of a single biogeographic constrain rendered overlapping age posterior distributions except when only the age of La Palma was used as age constraint, which rendered significantly younger ages (not shown).

Table 4
List of Bayesian analyses constrained under different molecular clocks, partition schemes, and diversification models ranked by Bayes Factors. Marginal likelihoods were estimated using a path-sampling method which values were used to calculate Bayes Factors. Data was either partitioned as four partitions (1st codon, 2nd codon, 3rd codon plus strand, 3rd codon minus strand), three partitions (1st, 2nd, 3rd), or two partitions (1st + 2nd, 3rd). Abbreviations: UCLN (uncorrelated log-normal clock), RLC (random local clock), and strict (strict clock).

Scheme and model	Marginal Ln	Bayes factors
4 partitions 3 UCLN Yule	−162220.017	0.000
4 partitions 3 UCLN Bith-Death	−162235.267	−30.499
4 partitions 4 UCLN Birth-Death	−162237.696	−35.357
4 partitions 4 UCLN Yule	−162243.669	−47.304
4 partitions 3 RLC Yule	−162302.005	−163.976
4 partitions 4 RLC Yule	−162331.782	−223.529
4 partitions 2 UCLN Yule	−162416.241	−392.448
4 partitions 4 strict Yule	−162441.814	−443.593
4 partitions 3 strict Yule	−162450.010	−459.986
3 partitions 3 UCLN Yule	−163814.156	−3188.278
4 partitions 1 UCLN Yule	−164341.140	−4242.246
2 partitions 2 UCLN Yule	−164447.132	−4454.230
Excluding 3rd codon sites		
2 partitions 1 UCLN Yule	−63545.708	0.000
2 partitions 2 UCLN Yule	−63605.540	−119.663
2 partitions 2 RLC Yule	−63637.950	−184.484
2 partitions 1 RLC Yule	−63833.142	−574.87

The mean substitution rate estimated for the combined 13 mitochondrial PCGs was 2.23×10^{-2} per site, million years and lineage, with a 95% confidence interval with a minimum of 1.99×10^{-2} and a maximum of 2.65×10^{-2}. This value corresponds to a pairwise

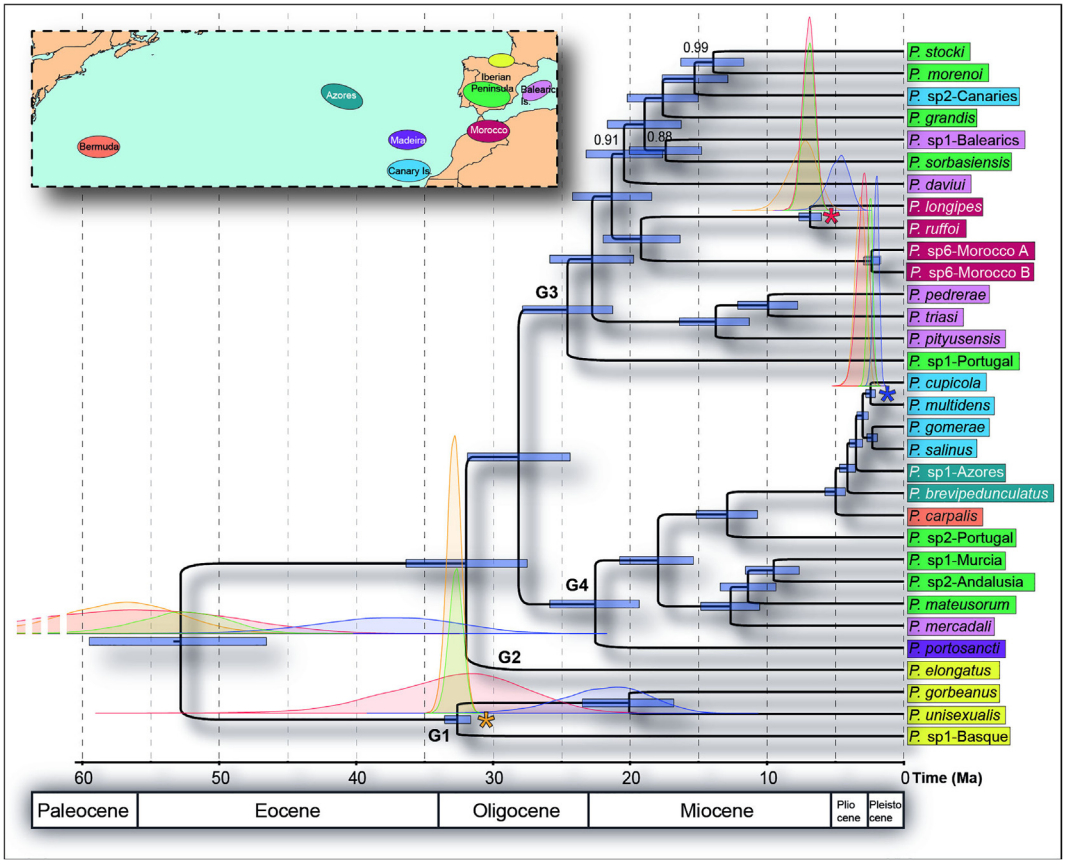

Fig. 4. Chronogram showing divergence times for *Pseudoniphargus* species estimated from the Bayesian analysis of the 13 mitochondrial protein-coding genes implementing the best selected partition, nucleotide substitution and clock models (see Tables 3 and 4 for details). Bars across nodes represent the 95% highest probability density intervals for the estimation of node ages. Three geologic events were used as aged constraints (indicated with asterisks in the tree). Distribution in orange represent values estimated using the Basque Country age of emergence, in red using as constrain the age of the Southern Riffian Corridor, while in blue using the emergence of La Palma island (see text). Distributions in green are values obtained when using the three constrains at the same time as priors. Posterior Bayesian credibility support values are indicated in nodes with values lower than 1.0. G1-G4 indicate the four main groups found in the *Pseudoniphargus* species studied.

divergence of 4.46%, nearly doubling the commonly implemented value of 2.3% (Brower, 1994). The mean substitution rate for first, second and third codon sites were estimated as 0.72×10^{-2} (0.64–0.81), 0.33×10^{-2} (0.29–0.37) and 5.65×10^{-2} (4.99–6.35), respectively. As expected, rate in third codon sites was about 10-fold higher than those estimated in first and second codon sites and also showed larger confidence intervals.

4. Discussion

4.1. Species boundaries and species delimitation methods

A preliminary morphology-based assessment of the species diversity present in our *Pseudoniphargus* samples enabled the assignment of specimens to a minimum of 30 already known described species plus other 17 presumably new. Results of three different methods of species delineation based on single-locus (*cox1*) data performed on the same set of specimens (two of them based on gene trees and one on distance matrices) showed a general agreement with the morphological analysis (Table 1; Fig. 2). Two of the presumed new species revealed by molecular delimitation methods (*Pseudoniphargus* sp1-Basque and *P.* sp1-Balearics) were confirmed morphologically afterwards, constituting an instance of "inadequate taxonomy revealed through the application of molecular methods" (Astrin et al., 2012). In other cases of presumably new species, morphological divergence was not recognizable or character states were too variable as to enable a formal taxonomic description based solely on morphological features. These cases may represent either evolutionarily young lineages in which incipient speciation is currently ongoing in absence of detectable morphological differentiation, or cryptic and reproductively isolated old lineages that deserve an appropriate taxonomic treatment (Delić et al., 2017).

Four possible cryptic species complexes were revealed in our study. The densely sampled *P. gorbeanus* appears split into two to three independently evolving lineages occurring in sympatry at Alava (N Spain). However, when using the more stringent criterion of only accepting GMYC or PTP highly-supported MOTUs, only GMYC favors the presence of two entities while the other methods concur in considering *P. gorbeanus* as a single species (Table 1; Fig. 2). Seemingly, *Pseudoniphargus elongatus* was divided into a minimum of two and a maximum of four highly supported cryptic allopatric lineages depending on the method used (Table 1; Fig. 2). Since a high number of individuals were sequenced in both species, these presumed cryptic lineages could be just a byproduct of sampling bias (Fujisawa and Barraclough, 2013; Zhang et al., 2013). Nevertheless, other species that were also densely sampled in our study –such as *P. multidens* and *P. portosancti*– were not split into different entities by the same analyses. Crypticism was also disclosed for the Menorcan and Mallorcan lineages of *P. mercadali* (Balearic Islands), showing at least two highly supported entities. The same pattern was found in *P. brevipedunculatus* on three Azores Islands (São Miguel, Faial and Pico), suggesting the occurrence of incipient allopatric speciation in absence of morphological divergence. Similar results have been reported in other insular stygobiont amphipods and thermosbaenaceans (Bauzà-Ribot et al., 2011; Cánovas et al., 2016). In contrast with the former cases of species crypticism, we found two cases

of sympatric species where members of each pair were clearly differentiated by diagnostic morphological features (i.e. *P. guernicae* and P. sp1-Basque in the Iberian northern clade G1, and the Bermudian *P. carpalis* and *P. grandimanus* in clade G4) but they were not distinctly supported as molecular MOTUs, likely due to very low inter- and intraspecific genetic divergences. GMYC has been shown to produce more entities than other methods, resulting in an overestimation of species numbers. This is usually due to low genetic divergence between lineages with the overlap of inter- and intraspecific divergences, or lack of reciprocal monophyly between sister clades (Hendrich et al., 2010; Talavera et al., 2013; Kekkonen et al., 2015). Nevertheless, the GMYC method seems to be better suited for detecting early speciation events, where both intra- and interspecific distances are low, as it is able to detect entities with lower intra-MOTU distances than PTP or other methods. The limitations associated to *cox1* polymorphisms and a single population-to-species threshold suppose that eventual occurrence of cases of split and lump of species are to be expected, so failures in identification are likely to occur if species are delimited based on molecular delimitation approaches only (Talavera et al., 2013). For that reason, GMYC and other molecular delimitation methods should be supplemented with additional information (i.e. morphological features) and should also take into account support values for defined MOTUs (i.e. assessing both uncertainties in tree topology and the support obtained by different coalescent models in GMYC) (Talavera et al., 2013; Fujisawa and Barraclough, 2013).

4.2. Mitogenome phylogenetics and biogeographic patterns

Our phylogenetic analysis shows the family Pseudoniphargidae to be at least Early Tertiary in age (Fig. 4). The family experienced a first major split during the Paleocene, when a branch (Clade G1) leading to the current Basque Country species diverged from the rest of pseudoniphargids. The occupation of continental waters by members of this Basque clade, assuming it was coeval to species diversification (Stock, 1980), could not take place before the end of the Eocene (about 40 Ma), when the current Basque area started to emerge from the sea (Plaziat, 1981; Rögl, 1998).

The remaining *Pseudoniphargus* experienced three further major splits, of which the more basal (Clade G2) led to *P. elongatus*, a species from the northern Spanish provinces of Santander and Burgos, adjacent to the Basque Country. This split was virtually synchronous with the first occupation of continental waters by the Basque lineage and might have resulted from the same episodes of marine regression affecting the southern coastline of the Gulf of Biscay at the late Eocene or Early Oligocene (Plaziat, 1981; Rögl, 1998).

During the Oligocene, the rest of *Pseudoniphargus* diverged in two clades (Fig. 4). One (Clade G3) comprises 13 species from southern Spain (Andalusia), Morocco and the Balearic Islands, plus one species each from Portugal and Gran Canaria (Canaries). The other one (Clade G4) includes eight species from the Canaries, Madeira, Azores and Bermuda, plus two from Portugal and one each from Andalusia, Murcia (SE Spain) and the Balearics. The most basal species in both clades correspond to Atlantic taxa –from Portugal in Clade G3; from Porto Santo Island (Madeira) in Clade G4– which, combined with the Atlantic condition of Clades G1 & G2, suggesting that the origin of the family Pseudoniphargidae should be located on that ocean. The occupation of the Mediterranean by pseudoniphargids seems thus to be a relatively recent episode in the evolutionary history of the group.

Only the three species from the Basque Country and the four species from Morocco –aside the monospecific Clade G2– conform monophyla with a clearly delimited geographical projection, denoting occupation of these areas was performed only once and by members of a single lineage (Fig. 3; Fig. 4). In the rest of territories, the *Pseudoniphargus* assemblage is polyphyletic, indicating these areas accumulate remnants of several colonization waves. Thus, the Balearic Islands harbor representatives of four independent lineages, whereas the Atlantic islands, Portugal and southern Spain include three each.

Comparison between the reported known ages of emergence of the oceanic islands harboring *Pseudoniphargus* and the estimated age of the corresponding nodes in our dated cladogram of species relationships shows a close correspondence in the cases of the species from Porto Santo (Madeira), Gran Canaria (Canaries) and Sao Miguel (Azores), suggesting colonization of inland waters and speciation on these islands took place as soon as emerged land was available. Island and node ages were found to be compatible also in the case of Bermuda and La Gomera, though in both cases the islands seem to have been colonized long afterwards they were exposed subaerially (but see below). Only the species from Faial Island (Azores) and El Hierro (Canaries) show an estimated age that is noticeably older than the islands harboring them, and only in the former case is this difference noticeable. Interestingly, the species from El Hierro inhabits only brackish-water coastal wells and has never been reported from fresh, inland groundwater, denoting it is still in the first steps of the colonization process of emerged land.

The presence of *Pseudoniphargus* on Porto Santo Island (Madeira) and Gran Canaria (Canaries) can be explained without recourse to long-range transoceanic dispersal. Assuming their ancestors were shallow-water marine species associated to submerged island primordials, the area currently comprised between both islands and the Iberian Peninsula has harbored seamounts and now drowned archipelagos since the early Tertiary (Fernández-Palacios et al., 2011). These structures might have acted as stepping-stones in the past, enabling the movement of species from the Iberian coasts.

On the contrary, the estimated age and genealogical affiliation of the rest of *Pseudoniphargus* species in this oceanic clade, which conform a well-established monophylum sister to a Portuguese species, suggest recent episodes of long-range transoceanic dispersal have played a major role in the establishment of their distribution pattern. Thus, Bermuda conforms a mid-plate rise in an area devoid of adjacent seamounts or ridges that might have acted as stepping-stones to enable its colonization. The lavas that formed the original Bermuda shield volcano are dated at 47–40 Ma, whereas at 40–36 Ma the Bermuda platform had already risen to sea level (Vogt and Jung, 2007). Notwithstanding that, the island has probably been submerged repeatedly since then, for the last time during the Pleistocene (Olson and Hearty, 2003). Hence the occupation of the freshwater habitats of the island by *Pseudoniphargus* is surely much more recent that the age attributed to the Bermudian lineage, and in accord with this is the fact (already remarked in the case of the species from El Hierro) that the Bermudian species is eurihaline, denoting its recent origin (Stock et al., 1986). The primordial Bermuda was already placed far away from the East Atlantic coast when it started its existence, and despite this, the estimated age of the *Pseudoniphargus* lineage present on the island is of only 5 Ma. Furthermore, this lineage occupies a basal position within its insular Atlantic clade (Fig. 3; Fig. 4) where the estimated species age diminishes in a Bermuda-Azores-Canaries progression. This could be explained by an episode of “reverse migration” back to the east Atlantic coast once Bermuda had been reached by the ancestor of this lineage. Considering this set of circumstances, it is hardly tenable that the opening of the Atlantic had played any role in the establishment of the current amphi-Atlantic distribution of *Pseudoniphargus*.

Whereas in the foregoing lineage from the Atlantic islands species diversification started in the Pliocene, most diversification in the peri-Mediterranean area took place in early Miocene to Tortonian times. During that period, the territory currently corresponding to southern Iberia, northern Morocco and the Balearics has evolved from a broad seaway between the Atlantic and the Mediterranean to a mosaic of islands and interior and marginal basins (Rögl, 1998; Martín et al., 2014; Achalhi et al., 2016). This scenario might have enabled species diversification associated to recurrent episodes of marine transgression and regression.

4.3. Conclusion

The data presented herein show the power of combining an extensive sampling across the distribution range of a lineage coupled with species delimitation methods and a phylogeny built from mitochondrial genomes to shed light on the species diversity, phylogenetic relationships and biogeographic history of a lineage of subterranean amphipods. Four possible cryptic species complexes hidden each within the formally recognized species *Pseudoniphargus gorbeanus*, *P. elongatus*, *P. mercadali* and *P. brevipedunculatus* have been identified in our study, while morphological characters and molecular delimitation methods delineated most of remaining species concomitantly. The obtained mitogenome-based phylogeny supports an origin of the genus *Pseudoniphargus* in the Early Tertiary, and the existence of four major clades, of which two show a clear limited geographical projection in the N Iberian Peninsula. The rest of the area of distribution was colonized multiple times in a complex pattern. Both vicariance and dispersal have contributed to the present distribution of *Pseudoniphargus,* but the opening of the Atlantic Ocean in the Mesozoic has not played any discernible role in the diversification and present biogeography of the genus.

Acknowledgements

This work was supported by the Spanish MINECO grants CGL2009-08256, CGL2012- 33597 and CGL2016-76164-P, financed by the Agencia Española de Investigación, (AEI) and the Euroean Regional Development Fund (FEDER). We thank the following colleagues for supplying *Pseudoniphargus* samples: Ana Sofía Reboleira (Copenhagen); Manuel Naranjo and Sonia Martín (Gran Canaria); Toni Pérez Fernández (Villacarrillo); Manuel Baena (Córdoba); Ana I. Camacho (Madrid); Andrés Ros (Murcia); Kenneth Meland (Bergen); and Mohammed Yacoubi (Marrakech). In the Azores, special thanks are extended to Isabel Amorim and Fernando Pereira (Terceira); Paulino Costa (Pico); and Teófilo Braga, Emanuel Pacheco, Manuel Soares, Cassilda Medeiros, Rita Pinheiros, José P. Medeiros and SINAGA S.A. (São Miguel).

Appendix A. Supplementary material

Supplementary data associated with this article can be found, in the online version, at https://doi.org/10.1016/j.ympev.2018.07.002.

References

Achalhi, M., Münch, P., Cornée, J.-J., Azdimousa, A., Melinte-Dobrinescu, M., Quillévéré, F., Drinia, H., Fauquette, S., Jiménez-Moreno, G., Merzeraud, G., Ben Moussa, A., El Kharim, Y., Feddi, N., 2016. The late miocene mediterranean-Atlantic connections through the North Rifian Corridor: New insights from the Boudinar and Arbaa Taourirt basins (northeastern Rif, Morocco). Palaeogeogr. Palaeoclimatol. Palaeoecol. 459, 131–152.

Astrin, J.J., Stüben, P.E., Misof, B., Wägele, J.W., Gimnich, F., Raupach, M.J., Ahrens, D., 2012. Exploring diversity in cryptorhynchine weevils (Coleoptera) using distance-, character- and tree-based species delineation. Mol. Phylogenet. Evol. 63, 1–14.

Baele, G., Lemey, P., Bedford, T., Rambaut, A., Suchard, M.A., Alekseyenko, A.V., 2012. Improving the accuracy of demo- graphic and molecular clock model comparison while accommo- dating phylogenetic uncertainty. Mol. Biol. Evol. 29, 2157–2167.

Barr, T.C., Holsinger, J.R., 1985. Speciation in cave faunas. Annu. Rev. Ecol. Syst. 16, 313–337.

Bauzà-Ribot, M.M., Jaume, D., Fornòs, J., Juan, C., Pons, J., 2011. Islands beneath islands: phylogeography of a groundwater amphipod crustacean in the Balearic archipelago. BMC Evol. Biol. 11, 221.

Bauzà-Ribot, M.M., Juan, C., Nardi, F., Oromí, P., Pons, J., Jaume, D., 2012. Mitogenomic phylogenetic analysis supports continental-scale vicariance in subterranean thalassoid crustaceans. Curr. Biol. 22, 1–6.

Bernt, M., Donath, A., Jühling, F., Externbrink, F., Florentz, C., Fritzsch, G., Pütz, J., Middendorf, M., Stadler, P.F., 2013. MITOS: improved de novo metazoan mitochondrial genome annotation. Mol. Phylogenet. Evol. 69, 313–319.

Blanco, L., Bernad, A., Lázaro, J.M., Martín, G., Garmendia, C., Salas, M., 1989. Highly efficient DNA synthesis by the phage phi 29 DNA polymerase. Symmetrical mode of DNA replication. J. Biol. Chem. 264, 8935–8940.

Boisvert, S., Laviolette, F., Corbeil, J., 2010. Ray: simultaneous assembly of reads from a mix of high-throughput sequencing technologies. J. Comput. Biol. 17, 1519–1533.

Bolger, A.M., Lohse, M., Usadel, B., 2014. Trimmomatic: a flexible trimmer for Illumina sequence data. Bioinformatics 30 (15), 2114–2120.

Botello, A., Iliffe, T.M., Alvarez, F., Juan, C., Jaume, D., 2013. Historical biogeography and phylogeny of *Typhlatya* cave shrimps (Decapoda: Atyidae) based on mitochondrial and nuclear data. J. Biogeogr. 40, 594–607.

Boutin, C., Coineau, N., 1990. “Regression model”, “Modèle biphase” d’évolution et origine des microorganismes stygobies interstitiels continentaux. Rev. Micropaléontol. 33, 303–322.

Brower, A.V.Z., 1994. Rapid morphological radiation and convergence among races of the butterfly Heliconius erato inferred from patterns of mitochondrial DNA evolution. Proc. Natl. Acad. Sci. U.S.A. 91, 6491–6495.

Bréhier, F., Jaume, D., 2009. A new species of *Pseudoniphargus* (Crustacea, Amphipoda, Melitidae) from an anchialine cave on the French Mediterranean coast. Zoosystema 31, 17–32.

Cánovas, F., Jurado-Rivera, J.A., Cerro-Gálvez, E., Juan, C., Jaume, D., Pons, J., 2016. DNA barcodes, cryptic diversity and phylogeography of a W Mediterranean assemblage of thermosbaenacean crustaceans. Zoolog. Scr. 45, 659–670.

Carracedo, J.C., Badiola, E.R., Guillou, H., de la Nuez, J., Pérez Torrado, F.J., 2001. Geology and volcanology of La Palma and El Hierro, western Canaries. Estud. Geol. 57, 175–273.

Castresana, J., 2000. Selection of conserved blocks from multiple alignments for their use in phylogenetic analysis. Mol. Biol. Evol. 17, 540–552.

Copilaş-Ciocianu, D., Fišer, C., Borza, P., Petrusek, A., 2018. Is subterranean lifestyle reversible? Independent and recent large-scale dispersal into surface waters by two species of the groundwater amphipod genus *Niphargus*. Mol. Phylogenet. Evol. 119, 37–49.

Delić, T., Svara, V., Coleman, C.O., Trontelj, P., Fišer, C., 2017. The giant cryptic amphipod species of the subterranean genus *Niphargus* (Crustacea, Amphipoda). Zoolog. Scr. 46, 740–752.

Drummond, A.J., Rambaut, A., 2007. BEAST: Bayesian evolutionary analysis by sampling trees. BMC Evolutionary Biol. 7.

Edgar, R.C., 2004. MUSCLE: multiple sequence alignment with high accuracy and high throughput. Nucleic Acids Res. 32, 1792–1797.

Ezard, T., Fujisawa, T.T.B., 2009. SPLITS: SPecies LImits by Threshold Statistics. version 1. R Package.

Feijão, P.C., Neiva, L.S., Azeredo-Espin, A.M.L., Lessinger, A.C., 2006. AMiGA: The arthropodan mitochondrial genomes accessible database. Bioinformatics 22, 902–903.

Fernández-Palacios, J.M., de Nascimento, L., Otto, R., Delgado, J.D., García-del-Rey, E., Arévalo, J.R., Whittaker, R.J., 2011. A reconstruction of Palaeo-Macaronesia, with particular reference to the long- term biogeography of the Atlantic island laurel forests. J. Biogeography 38, 226–246.

Fišer, C., Robinson, C.T., Malard, F., 2018. Cryptic species as a window into the paradigm shift of the species concept. Mol. Ecol. 27, 613–635.

Folmer, O., Black, M., Hoeh, W., Lutz, R., Vrijenhoek, R., 1994. DNA primers for amplification of mitochondrial cytochrome c oxidase subunit I from diverse metazoan invertebrates. Mol. Mar. Biol. Biotech. 3, 294–299.

Fourment, M., Gibbs, M.J., 2006. PATRISTIC: a program for calculating patristic distances and graphically comparing the components of genetic change. BMC Evol. Biol. 6, 1.

Fujisawa, T., Barraclough, T.G., 2013. Delimiting species using single-locus data and the Generalized Mixed Yule Coalescent (GMYC) approach: a revised method and evaluation on simulated datasets. Syst. Biol. 62, 707–724.

Grabherr, M.G., Haas, B.J., Yassour, M., Levin, J.Z., Thompson, D.A., Amit, I., Adiconis, X., Fan, L., Raychowdhury, R., Zeng, Q., Chen, Z., Mauceli, E., Hacohen, N., Gnirke, A., Rhind, N., Di Palma, F., Birren, B.W., Nusbaum, C., Lindblad-Toh, K., Friedman, N., Regev, A., 2011. Full-length transcriptome assembly from RNA-Seq data without a reference genome. Nat. Biotechnol. 29, 644–652.

Hassanin, A., 2006. Phylogeny of Arthropoda inferred from mitochondrial sequences: Strategies for limiting the misleading effects of multiple changes in pattern and rates of substitution. Mol. Phylogenet. Evol. 38, 100–116.

Hendrich, L., Pons, J., Ribera, I., Balke, M., 2010. Mitochondrial Cox1 sequence data reliably uncover patterns of insect diversity but suffer from high lineage- idiosyncratic error rates. PLoS One 5 e14448.

Horton, T., Lowry, J., De Broyer, C., Bellan-Santini, D., Coleman, C.O., Daneliya, M., Dauvin, J.C., Fišer, C., Gasca, R., Grabowski, M., Guerra-García, J.M., Hendrycks, E., Holsinger, J., Hughes, L., Jaume, D., Jazdzewski, K., Just, J., Kamaltynov, R.M., Kim, Y.-H., King, R., Krapp-Schickel, T., LeCroy, S., Lörz, A.N., Senna, A.R., Serejo, C., Sket, B., Tandberg, A.H., Thomas, J., Thurston, M., Vader, W., Väinölä, R., Vonk, R., White, K., Zeidler, W., (Eds.), 2018. World Amphipoda Database. Pseudoniphargus Chevreux, 1901. Accessed through: World Register of Marine Species at: http://www.marinespecies.org/aphia.php?p=taxdetails&id=101682 on 20187-053-22.

Hou, Z., Li, S., 2017. Tethyan changes shaped aquatic diversification. Biol. Rev. https://doi.org/10.1111/brv.12376.

Jaume, D., 1991. Two new species of the amphipod genus *Pseudoniphargus* (Crustacea) from Cabrera (Balearic Islands). Stygologia 6, 177–189.

Jaume, D., Christenson, K., 2001. Amphi-Atlantic distribution of the subterranean amphipod family Metacrangonyctidae (Crustacea, Gammaridea). Contrib. Zool. 70, 99–125.

Jażdżewski, K., Grabowski, M., Kupryjanowicz, J., 2014. Further records of Amphipoda from Baltic Eocene amber with first evidence of prae-copulatory behaviour in a fossil amphipod and remarks on the taxonomic position of Palaeogammarus Zaddach, 1864. Zootaxa 3765, 401–417.

Jurado-Rivera, J.A., Pons, J., Alvarez, F., Botello, A., Humphreys, W.F., Page, T.J., Iliffe, T.M., Willassen, E., Meland, K., Juan, C., Jaume, D., 2017. Phylogenetic evidence that both ancient vicariance and dispersal have contributed to the biogeographic patterns of anchialine cave shrimps. Sci. Rep. 7, 2852.

Karaman, G.S., Ruffo, S., 1989. *Tyrrhenogammarus sardous*, new genus and species with description of several new taxa of genus *Pseudoniphargus* Chevreux, 1901 from Sicily (Amphipoda, Gammaridea). Animalia 19, 161–192.
Katoh, S., 2013. MAFFT multiple sequence alignment software version 7: improvements in performance and usability. Mol. Biol. Evol. 772–780.
Kekkonen, M., Mutanen, M., Kaila, L., Nieminen, M., Hebert, P.D.N., 2015. Delineating species with DNA barcodes: a case of taxon dependent method performance in moths. PLoS One 10 e0122481.
Lanfear, R., Calcott, B., Ho, S.Y.W., Guindon, S., 2012. Partitionfinder: combined selection of partitioning schemes and substitution models for phylogenetic analyses. Mol. Biol. Evol. 29, 1695–1701.
Lartillot, N., Philippe, H., 2004. A Bayesian mixture model for across-site heterogeneities in the aminoacid replacement process. Mol. Phylogenet. Evol. 21, 1095–1109.
Lartillot, N., Lepage, T., Blanquart, S., 2009. PhyloBayes 3: a Bayesian software package for phylogenetic reconstruction and molecular dating. Bioinformatics 25, 2286–2288.
Lefébure, T., Douady, C.J., Gouy, M., Trontelj, P., Briolay, J., Gibert, J., 2006. Phylogeography of a subterranean amphipod reveals cryptic diversity and dynamic evolution in extreme environments. Mol. Ecol. 15, 1797–1806.
Lefébure, T., Douady, C.J., Malard, F., Gibert, J., 2007. Testing dispersal and cryptic diversity in a widely distributed groundwater amphipod (*Niphargus rhenorhodanensis*). Mol. Phylogenet. Evol. 42, 676–686.
Martín, J.M., Puga-Bernabéu, A., Aguirre, J., Braga, J.C., 2014. Miocene Atlantic-Mediterranean seaways in the Betic Cordillera (Southern Spain). Revista de la Sociedad Geológica de España 27, 175–186.
Messouli, M., Messana, G., Yacoubi-Khebiza, M., 2006. Three new species of *Pseudoniphargus* (Amphipoda) from the groundwater of three Mediterranean islands, with notes on the *Ps. adriaticus*. Subterranean Biol. 4, 79–101.
Nguyen, L.T., Schmidt, H.A., von Haeseler, A., Minh, B.Q., 2015. IQ-TREE: A fast and effective stochastic algorithm for estimating maximum likelihood phylogenies. Mol. Biol. Evol. 32, 268–274.
Notenboom, J., 1986. The species of the genus *Pseudoniphargus* Chevreux, 1901 (Amphipoda) from Northern Spain. Bijdragen tot de Dierkunde 56, 75–122.
Notenboom, J., 1987a. Species of the genus *Pseudoniphargus* Chevreux, 1901 (Amphipoda) from the Betic Cordillera of Southern Spain. Bijdragen tot de Dierkunde 57, 87–150.
Notenboom, J., 1987b. Lusitanian species of the amphipod *Pseudoniphargus* Chevreux, 1901 with a key to all known Iberian species. Bijdragen tot de Dierkunde 57, 191–206.
Notenboom, J., 1988. Phylogenetic relationships and biogeography of the groundwater-dwelling amphipod genus *Pseudoniphargus* (Crustacea), with emphasis on the Iberian species. Bijdragen tot de Dierkunde 58, 159–204.
Notenboom, J., 1991. Marine regressions and the evolution of groundwater dwelling amphipods (Crustacea). J. Biogeogr. 18, 437–454.
Nylander, J.A.A., 2004. MrAIC.pl v1.4.6. Evolutionary Biology Centre, Uppsala University.
Pfenninger, M., Schwenk, K., 2007a. Cryptic animal species are homogeneously distributed among taxa and biogeographical regions. BMC Evol. Biol. 7, 21.
Olson, S.L., Hearty, P.J., 2003. Probable extirpation of a breeding colony of Short-tailed Albatross (Phoebastria albatrus) on Bermuda by Pleistocene sea-level rise. Proc. Natl. Acad. Sci. 100, 12825–12829.
Pfenninger, M., Schwenk, K., 2007b. Cryptic animal species are homogeneously distributed among taxa and biogeographical regions. BMC Evol. Biol. 7, 121.
Plaziat, J.C., 1981. Late cretaceous to late eocene palaeogeographic evolution of southwest Europe. Palaeogeogr. Palaeoclimatol. Palaeoecol. 36, 263–320.
Pons, J., Barraclough, T.G., Gómez-Zurita, J., Cardoso, A., Duran, D.P., Hazell, S., Kamoun, S., Sumlin, W.D., Vogler, A.P., 2006. Sequence-based species delimitation for the DNA taxonomy of undescribed insects. Syst. Biol. 55, 595–609.
Pons, J., Bauzà-Ribot, M., Jaume, D., Juan, C., 2014. Next–generation sequencing, phylogenetic signal and comparative mitogenomic analyses in Metacrangonyctidae (Amphipoda: Crustacea). BMC Genomics 15, 566.
Puillandre, N., Lambert, A., Brouillet, S., Achaz, G., 2012. ABGD, automatic barcode gap discovery for primary species delimitation. Mol. Ecol. 21, 1864–1877.
Rambaut, A., Suchard, M.A., Xie, D., Drummond, A.J., 2015. Tracer v1.6. Available via http://beast.bio.ed.ac.uk/Tracer.
Rögl, F., 1998. Palaeogeographic considerations for Mediterranean and Paratethys seaways (Oligocene to Miocene). Annalen des Naturhistorischen Museums in Wien 99A, 279–310.
Schattner, P., Brooks, A.N., Lowe, T.M., 2005. The tRNAscan–SE, snoscan and snoGPS web servers for the detection of tRNAs and snoRNAs. Nucl. Acids Res. 33, W686–W689.
Stamatakis, A., Ludwig, T., Meier, H., 2005. Raxml-iii. A fast program for maximum likelihood-based inference of large phylogenetic trees. Bioinformatics 21, 456–463.
Starr, H.W., Hegna, T.A., McMenamin, M.A.S., 2016. Epilogue to the tale of the Triassic amphipod: Rosagammarus McMenamin, Zapata and Hussley, 2013 is a decapod tail (Luning Formation, Nevada, USA). J. Crustac. Biol. 36, 525–529.
Stock, J.H., 1977. The taxonomy and zoogeography of the hadziid Amphipoda. Studies on the Fauna of Curaçao and other Caribbean Islands 55, 1–130.
Stock, J.H., 1980. Regression model evolution as exemplified by the genus *Pseudoniphargus* (Amphipoda). Bijdragen tot de Dierkunde 50, 105–144.
Stock, J.H., 1993. Some remarkable distribution patterns in stygobion Amphipoda. J. Nat. Hist. 27, 807–819.
Stock, J.H., Abreu, A.D., 1992. Three new species of *Pseudoniphargus* (Crustacea: Amphipoda) from the Madeira archipelago. Boletim do Museu Municipal do Funchal 44, 131–155.
Stock, J.H., Holsinger, J.R., Sket, B., Iliffe, T.M., 1986. Two new species of *Pseudoniphargus* (Amphipoda), in Bermudian groundwaters. Zoolog. Scr. 15, 237–249.
Stokkan, M., Jurado-Rivera, J.A., Juan, C., Jaume, D., Pons, J., 2016. Mitochondrial genome rearrangements at low taxonomic levels: three distinct mitogenome gene orders inthe genus *Pseudoniphargus* (Crustacea: Amphipoda). Mitochondrial DNA 27, 3579–3589.
Stokkan, M., Pérez-Fernández, A., Baena, M., Jaume, D., 2018. Two new species of *Pseudoniphargus* (Amphipoda: Pseudoniphargidae) from southern Spain. Zootaxa 4418, 264–280.
Swofford, D., 2002. PAUP*: Phylogenetic Analysis using Parsimony* (and other methods), 4.0b10. Sinauer Associates, Sunderland, MA.
Talavera, G., Dincă, V., Vila, R., 2013. Factors affecting species delimitations with the GMYC model: insights from a butterfly survey. Methods Ecol. Evol. 4, 1101–1110.
Vogt, P.R., Jung, W.-Y., 2007. Origin of the Bermuda volcanoes and the Bermuda Rise: History, observations, models, and puzzles. Geol. Soc. Am. Special Pap. 430, 553–591.
Wagner, H.P., 1994. A monographic review of the Thermosbaenacea (Crustacea: Peracarida). A study on their morphology, taxonomy, phylogeny and biogeography. Zoologische Verhandelingen 29, 1–338.
Witt, J.D.S., Hebert, P.D.N., 2000. Cryptic species diversity and evolution in the amphipod genus *Hyalella* within central glaciated North America: a molecular phylogenetic approach. Can. J. Fish. Aquat. Sci. 57, 687–698.
Witt, J.D.S., Threloff, D.L., Hebert, P.D.N., 2006. DNA barcoding reveals extraordinary cryptic diversity in an amphipod genus: Implications for desert spring conservation. Mol. Ecol. 15, 3073–3082.
Xia, X., Lemey, P., 2009. Assessing substitution saturation with DAMBE. In: Lemey, Philippe, Salemi, Marco, Vandamme, Anne-Mieke (Eds.), The Phylogenetic Handbook: A Practical Approach to DNA and Protein Phylogeny, second ed. Cambridge University Press, pp. 615–630.
Xia, X., Xie, Z., Salemi, M., Chen, L., Wang, Y., 2003. An index of substitution saturation and its application. Mol. Phylogenet. Evol. 26, 1–7.
Zhang, J., Kapli, P., Pavlidis, P., Stamatakis, A., 2013. A general species delimitation method with applications to phylogenetic placements. Bioinformatics 29, 2869–2876.